QUANTIFYING THE LATITUDINAL DISTRIBUTION OF VOLATILE-RELATED LANDFORMS ON MARS' SOUTHERN HEMISPHERE, TERRA CIMMERIA. M. Voelker[1], E. Hauber[2], A. Cardesín-Moinelo[1], P. Martin[1], [1]European Space Agency, European Space Astronomy Center, Camino Bajo del Castillo s/n, Villanueva de la Cañada, E-28692 Madrid, Spain (martin.voelker@esa.int), [2]German Aerospace Center, Institute of Planetary Research, Rutherfordstr. 2, D-12489 Berlin, Germany.

Introduction: As a part of a global study [1-6], we applied the so-called grid-mapping method to quantify the geography of given landforms on Mars' southern hemisphere. The study areas comprise Terra Cimmeria (TC, presented here, Fig. 1), as well as Noachis Terra (NT) [7], and Terra Sirenum (TS, TBD).

Grid-mapping allows to map extensive areas with efficiency and an increased level of objectivity [2-5], revealing relations between spatial distribution and morphologies which are only visible from a wider perspective. Thus, we studied the distribution of possibly water- and ice-related landforms over a 100 km-wide area extending from the equator to the south pole to derive information about the latitude-dependence of landforms and the responsible climatic control.

Methods: The grid-mapping approach is based on a tick box system, overlaying various remote sensing datasets. It requires a multi-layer GIS-environment in order to combine both remote sensing imagery and a polygonal vector shapefile containing the grid boxes (each 20×20 km; Cassini-projected map). Every box is being investigated for the presence or absence of 28 pre-selected landforms. This approach is able to increase the level of intersubjectivity, as it is based on simple "Yes" and "No" decisions of the mapper. Hence it is possible for every reader to follow each of the mapper's decisions. Mapping scale was 1:25,000 and is based on CTX imagery [8] and TES for albedo [9].

The research area is a 100 km wide swath extending from the equator (centered along 135°E, Fig. 1) to the south polar cap. The study area has been selected as it consists of a representative portion of the southern cratered highlands without any other significant large topographical or geological feature in its vicinity that might influence the distribution of landforms.

Results: We were able to detect 26 of the 28 preselected landforms. Due to the large number of landforms we are focusing on the results of 16 landforms, which can be generally classified into aeolian, fluvial, periglacial, and glacial features/processes. The selection focuses on landforms being formed by exogenic processes, and hence, being climatic indicators, e.g., wind or precipitation.

Aeolian: Landforms being formed by wind: dunes, transversal aeolian ridges (TARs), ripples, dust. These landforms are mainly found in the lower latitudes (≤45°S; Fig. 2), and rarely at higher latitudes.

Fluvial: Landforms being formed by liquid water: dendritic channels [10]. Due to the possibly ambiguous origin of some channel types (e.g., lava vs. water), we only classified dendritic channels as fluvial. They are mainly found in low to mid latitudes (Fig. 2); south of 70°S they lack entirely.

Periglacial: Landforms that are likely related to (sub)surface ice deposits [11-14]: latitude-dependent mantle (LDM), scalloped terrain, viscous-flow features, polygons, gullies, pedestal craters, palimpsests. They are mostly found within the mid-latitudes (30-60°S, Fig. 2) but also in the high latitudes (60-85°S), albeit to a smaller extent.

Glacial (polar): Landforms that are being formed and characterized by surface ice deposits (both H_2O and CO_2 ice) [15,16]: polar deposits, polar pits, dark material/spiders. They only occur south of 65°S (Fig. 2). In contrast to NT [7], we could not detect two distinctive polar deposit layers in TC.

Sublimation: Besides the four geomorphologic domains, the dataset also allowed a reclassification into other processes, like sublimation [17] (Fig. 3). This class considers all landforms that are assumed to be formed by sublimation processes of H_2O and CO_2 deposits (scalloped terrain, small pits, polar pits, dark material/spiders). It reveals general information about current climatic conditions that do not allow H_2O and CO_2 ice to be stable on the surface. Within the latitudes from 30°S to 70°S, sublimation features occur on ~8% of all grids; above 70°S they increase to 38-58%.

Discussion: Like in NT we were able to identify three different environments in TC (Fig. 2); (1) a dry zone (aeolian > periglacial) mostly devoid of volatiles within the low latitudes (0° to ~37°S); (2) a volatile-rich transitional zone (aeolian < periglacial > polar; probably dominated by water-ice) ranging from 37° to 72°S, showing slight sublimation activities; (3) a polar volatile-rich zone (polar > periglacial) probably dominated by permanent surface CO_2 ice deposits) extending from 72° to the pole. These environmental zones are similar in latitudinal extent to those found in NT.

In contrast to NT, the distribution of sublimation features is far more even; they occur on any latitude where volatiles exist in TC, however, in a generally lower density than in NT. Albedo has no influence on the distribution of sublimation features (Fig. 3). No albedo-temperature feedback has been detected based on the distribution of sublimation features. Sublimation

activities in TC show two distinctive intensity levels (Fig. 3); lower where LDM predominates (>30°S), and higher where polar deposits occur (>70°S). This might be caused by a larger influence of CO_2 at high latitudes, and its active cycle of deposition during winter, and removal during summer [18,19].

Future work: The third study area of TS will complete this project, and allow a final synthesis of all three study areas, and hence, the southern hemisphere in general. Thus, it is possible to quantify the landforms on a global scale, by juxtaposing the distribution of landforms from the southern hemisphere to the results obtained in the northern hemisphere [3-5].

References: [1] Ramsdale J.D. et al. (2017) PSS 140, 49-61. [2] Voelker M. et al. (2018) Icarus 307, 116. [3] Orgel C. et al. (2018) JGR. [4] Ramsdale J.D. et al. (2018) JGR. [5] Séjourné A. et al. (2018) JGR. [6] Voelker M. and Ramsdale J.D. (2019) in: Planetary Cartography and GIS, Ed. Hargitai H. [7] Voelker et al. (2019) 50th LPSC, #1776. [8] Malin M.C. et al. (2007) JGR 112, E05S04. [10] Carr M. (1996) Water on Mars, p.248. [11] Mustard J.F. et al. (2001) Nature 412, 411-414. [12] Kreslavsky M.A. and Head J.W. (2002) GRL 29 (15), 14-1-14-4. [13] Kostama V.-P. et al. (2006) GRL 33, L11201. [14] Conway S.J. and Balme M.R. (2014) GRL 41, 5402-5409. [15] Bibring J.-P. et al. (2004) Nature 428, 627-630. [16] Byrne S. (2009) Ann. Rev. Earth and Planet. Sci. 37, 535-560. [17] Mangold N. (2011) Geomorphology 126, 1-17. [18] Hess S.L. et al. (1979) JGR 84, 2923-2927. [19] Bierson C.J. et al. (2016) GRL 43, 4172-4179.

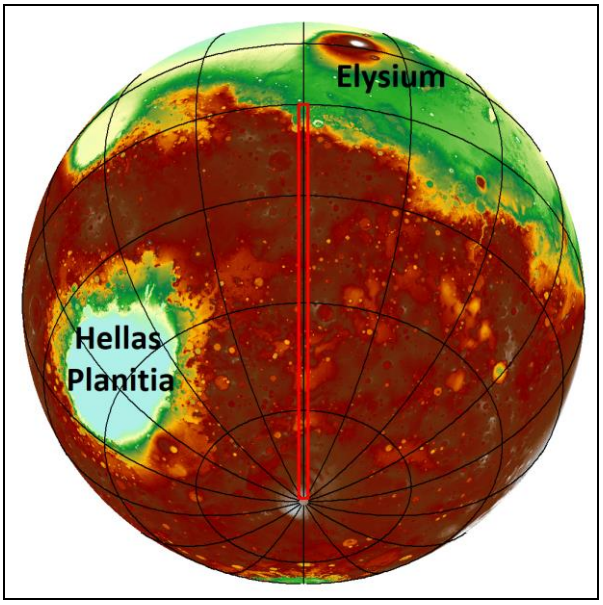

Fig. 1. *Study area (red box) in Terra Cimmeria, located along 135°E (MOLA).*

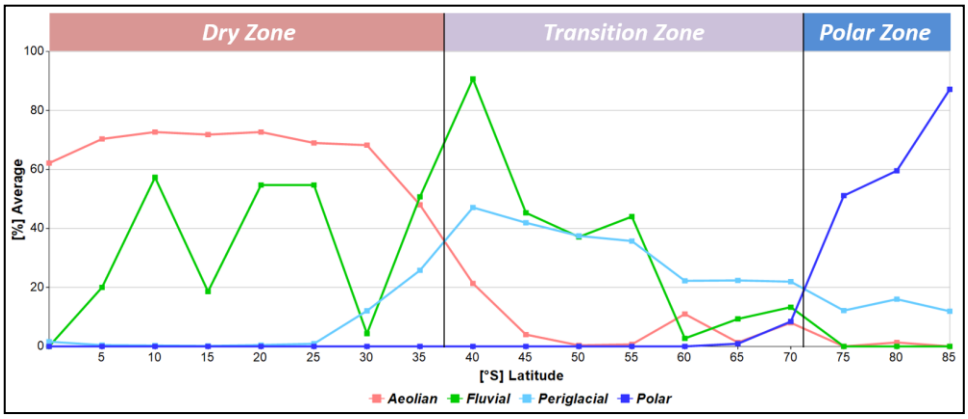

Fig. 2. *Suggested environmental zones in Terra Cimmeria. The presented %-values are averaged numbers of multiple landforms indicative for each geomorphological domain (see text for details)*

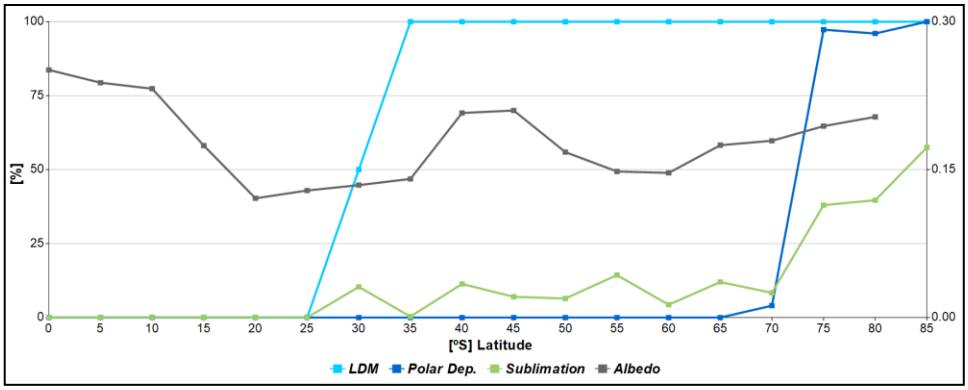

Fig. 3. *Distribution of volatile-rich layers (LDM, polar deposits; blue), and related sublimation features (green). Note that albedo (right axis, grey) has no influence of the distribution of sublimation features.*